International Journal of Robotics Research

Paper number: 375140

Please ensure that you have obtained and enclosed all necessary permissions for the reproduction of artistic works, e.g. illustrations, photographs, charts, maps, other visual material, etc.) not owned by yourself, and ensure that the Contribution contains no unlawful statements and does not infringe any rights of others, and agree to indemnify the Publisher, SAGE Publications Ltd, against any claims in respect of the above warranties and that you agree that the Conditions of Publication form part of the Publishing Agreement.

Author queries

Query	Author reply
Please supply a list of key words.	
Please cite Huntsberger et al. (2009), Ono et al. (2008), and Visentin and Venturini (1997) in the text or delete from the reference list.	
Please supply page range for Kawano et al. (2001), Visentin and Venturini (1997), and Whittaker et al. (2001).	

ijrr

The International Journal of
Robotics Research
00(000):1–12
©The Author(s) 2010
Reprints and permission:
sagepub.co.uk/journalsPermissions.nav
DOI: 10.1177/0278364910375140
ijr.sagepub.com

SAGE

A Kinematic Approach to Determining the Optimal Actuator Sensor Architecture for Space Robots

Peggy Boning and Steven Dubowsky*

Abstract

Autonomous space robots will be required for such future missions as the construction of large space structures and repairing disabled satellites. These robots will need to be precisely controlled. However, factors such as manipulator joint/actuator friction and spacecraft attitude control thruster inaccuracies can substantially degrade control system performance. Sensor-based control algorithms can be used to mitigate the effects of actuator error, but sensors can add substantially to a space system's weight, complexity, and cost, and reduce its reliability. Here a method is presented to determine the sensor architecture that uses the minimum number of sensors that can simultaneously compensate for errors and disturbance in a space robot's manipulator joint actuators, spacecraft thrusters, and reaction wheels. The placement and minimal number of sensors is determined by analytically structuring the system into "canonical chains" that consist of the manipulator links and spacecraft with force/torque sensors placed between the space robot's spacecraft and its manipulators. These chains are combined to determine the number of sensors needed for the entire system. Examples of one- and two-manipulator space robots are studied and the results are validated by simulation.

Keywords

1. Introduction

1.1. Motivation

Space robots will be required for a number of important future missions, such as the construction of large space structures for large space telescopes and space solar power stations and for the repair of disabled spacecraft (Kawano et al. 2001; Staritz et al. 2001; Whittaker et al. 2001; Oda et al. 2003; Shoemaker and Wright 2004; Lillie 2006). See Figure 1.

However, the precision of open-loop forces and torques for space manipulator actuators is poor. The lightweight motors with high-gear ratio drives and dry space-qualified lubricants result in robot joints and transmissions that have high non-linear Coulomb friction (Newman et al. 1992). This friction problem is particularly critical when the robots perform force-control tasks (Boning 2001).

The reaction thrusters used to control a free-flying robot's spacecraft attitude and position are also highly non-linear and imprecise. The thrusters are generally controlled with highly non-linear valves with pulse-width modulation (PWM) or pulse-width–pulse-frequency modulation (PWPFM) (Sidi 1997). These valves are sensitive to thermal changes and variations in the fuel supply level, etc., and hence their precision is quite poor. Reaction wheels for attitude control are more precise; however, they cannot control a robot's spacecraft position. For space robots to perform their future tasks, the degrading effects of imprecise manipulator and spacecraft actuation must be mitigated by their control systems.

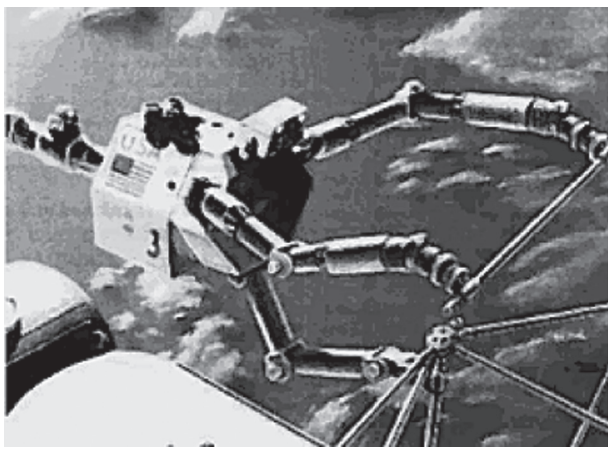

Fig. 1. A NASA concept of a multiarm space robot performing an on-orbit construction mission.

***Corresponding author:**
Steven Dubowsky
The MIT Field and Space Robotics Laboratory
The Massachusetts Institute of Technology
Cambridge, MA 02139, USA
fsrl@mit.edu

1.2. Control Background

A number of effective methods for imprecise actuation have been developed for conventional fixed-based manipulators, including sensor-based methods, adaptive compensation, and model-based methods. However, these methods are constrained by the challenges of space systems (Whittaker et al. 2001; Ueno et al. 2003).

Fixed-based adaptive control methods have been developed to estimate unknown joint actuator friction parameters (Slotine and Li 1987; de Wit 1988). However, adaptive control formulations can be complex, making their implementation difficult, especially for high-degree-of-freedom space systems (de Wit et al. 1995). In addition, these methods have not yet been extended to the identification of attitude control thruster forces and moments. Finally, for space systems, relying on measurement of uncertainty and errors rather than indirect computation is generally preferred, due to the wide range of environmental conditions that can affect system parameters and the need to avoid dangerous transient behavior during adaptation.

Model-based actuator effort compensation methods use mathematical models to predict actuator behavior (de Wit 1988). However, model-based compensation is not well suited to space robots because in the hostile environment of space, model parameters are very difficult to predict. Other methods based on special command profiles to deal with imprecise actuation have been developed, such as high-frequency dither (Ipri and Asada 1995). Again, these methods have yet to be developed for space applications, in particular for reaction thruster uncertainty.

When sensors are available at each system actuator, measurement-based closed-loop force or torque control can be used (Pfeffer et al. 1989; Vischer and Khatib 1995). This approach is desirable because it does not require detailed models or adaptation and is robust to system uncertainty and time-changing parameters.

However, for a space robot with multiple manipulators and multiple thrusters, sensor-based methods would require a relatively large number of sensors that clearly would increase cost, weight, and complexity, and reduce system reliability. Therefore, methods that use a small number of sensors to measure actuation outputs and use these measurements in closed-loop force/torque control to provide space robots precise control capabilities would be highly desirable. The focus of this work is to develop such methods.

1.3. Approach

Here a control method to compensate for poor actuation precision using a small number of sensors, called space base sensor control (SBSC), is presented (Boning and Dubowsky 2006a,b). We then present a method that determines, for a given system based on its kinematic configuration, the SBSC sensor architecture that uses a minimum number of sensors to simultaneously measure joint and spacecraft actuation of a space robot (Boning and Dubowsky 2006b).

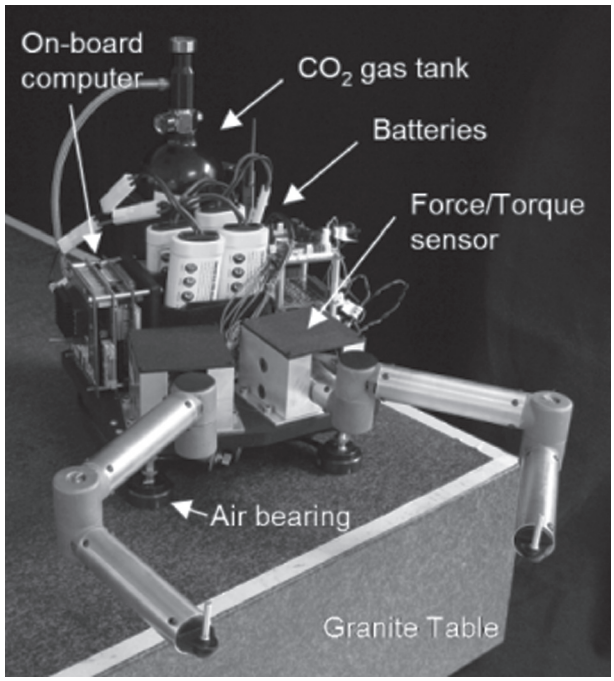

Fig. 2. An MIT laboratory free-flying space robot equipped with base force torque sensors.

SBSC is an extension of the base sensor control (BSC) method originally developed for fixed-based terrestrial robots (Morel and Dubowsky 1996, 1998; Morel et al. 2000). For space manipulators, the motions of the spacecraft and the torques of its attitude control system must be considered. The movement of a space robot's manipulator can disturb its spacecraft base and the control must take these disturbances into account (Dubowsky and Papadopoulos 1993).

Figure 2 shows a system equipped for SBSC. It is a free-flying laboratory space robot system for studying orbital robot control, including SBSC. The system has multiple two-manipulator robots that are supported by air bearings that float on a polished granite table. The robots have cold gas thrusters for attitude control and are self-contained with their own control computers, electronics, sensors, and gas supplies. As shown in the figure, there are force/torque sensors mounted at the base of the manipulators. Using the SBSC algorithm discussed below these sensors can be used to estimate the manipulator's joint actuator outputs while simultaneously estimating spacecraft thruster forces and moments. Owing to space limitations, a detailed description this system and its performance is beyond the scope of this paper, which instead focuses on the optimal sensor placement architecture and minimal number of sensors for a given systems design. The reader is referred to Boning (2009) and Boning et al. (2008) for the details of this system.

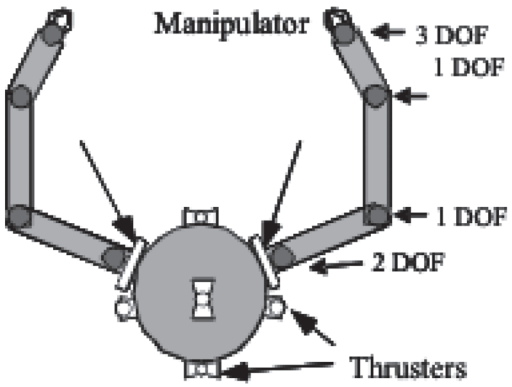

Fig. 3. A Conceptual Model of Multi-Manipulator Free-Flying Space Robot.

2. Analytical Development

2.1. System Description and Assumptions

The systems considered here are three-dimensional free-flying and free-floating space robots with multiple manipulators. Figure 3 shows a concept of a space robot with two manipulators. The sensors of the robot may include joint encoders, force/torque sensors, gyroscopes, inertial measurement units (IMUs), etc. The actuation may include joint motors, spacecraft thrusters, and reaction wheels.

In general, there might be p manipulators, each with n links. It is assumed that there is a six-axis force/torque sensor between each manipulator and its spacecraft. Manipulators are assumed to have rotary joints, but the method developed here can be extended to translational joints. It is also assumed that the spacecraft and links are 3D rigid bodies (fuel sloshing and flexible modes of the robot are not considered). The combined efforts of the thrusters and reactions wheels are represented by a force and moment applied at the center of mass of the spacecraft. Actuator forces and moments, friction at each joint, and reaction thruster forces are assumed to be poorly known. Further, it is assumed that there are no additional external loads acting on the system. Gravity gradient effects are neglected because they are small compared with the other forces. For this study, measurement noise is not considered, although it could be a significant factor and should be addressed in future studies. If the manipulator is holding a payload, a firm grasp by the end-effector is assumed.

As discussed in the following section, the SBSC and the force/torque sensors measurements can be used to identify the net torque output of the manipulator's actuators. The same measurements are used to identify spacecraft thruster outputs. Other measured quantities required are joint angles for each of the j manipulators ($\mathbf{q}^{(j)}$), linear acceleration of the spacecraft ($\dot{\mathbf{v}}_s = \ddot{\mathbf{r}}_s$), spacecraft orientation ($\boldsymbol{\theta}$), angular velocity of the spacecraft ($\boldsymbol{\omega}_s$), and angular acceleration of the spacecraft ($\dot{\boldsymbol{\omega}}_s$), as defined in Figure 4.

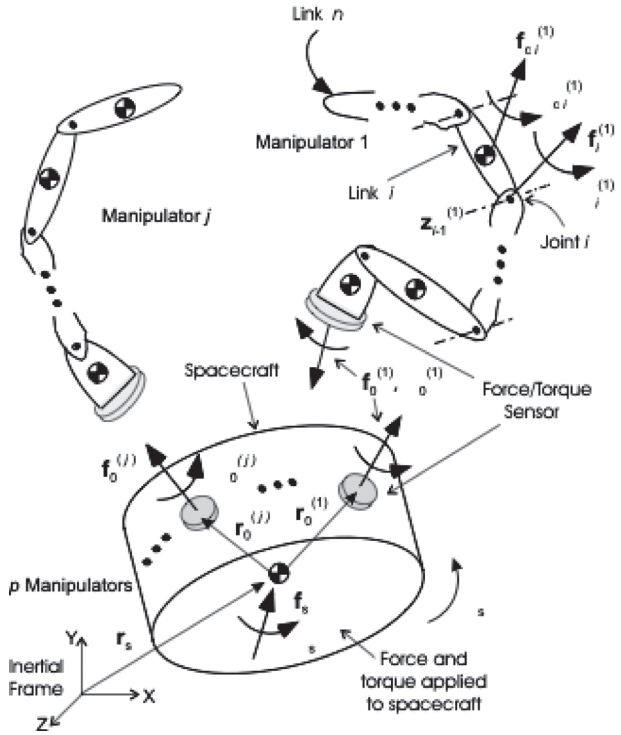

Fig. 4. System model with coordinates.

2.2. SBSC

As discussed above, the approach uses a method, called SBSC, to identify actuator efforts from a six-axis force/torque sensor placed between each manipulator and its spacecraft (see Figure 4). It is shown in the following that these sensors can simultaneously measure the system's manipulator actuator outputs the forces and torques applied to the spacecraft by its thruster reaction forces and reaction wheels (Boning and Dubowsky 2006a). The measurements can be used in inner force or torque control loops to eliminate torque and thruster actuation errors, including the effects of friction, improving the precision control system (see Figure 5). These sensors could also be used for continuous monitoring to detect degradation in actuator performance.

The equations for linear momentum $\mathbf{p}_s$ and angular momentum $\mathbf{H}_s$ at the center of mass of the spacecraft are

$$\begin{aligned} \mathbf{p}_s &= m_s \mathbf{v}_s, \\ \mathbf{H}_s &= \mathbf{I}_s\, \boldsymbol{\omega}_s, \end{aligned} \tag{1}$$

where $\mathbf{I}_s$ is the spacecraft inertia tensor and m_s is the spacecraft mass. From conservation of momentum, the time derivative of the momentum is equal to the forces and torques applied to the spacecraft:

$$\begin{aligned} \dot{\mathbf{p}}_s &= \sum \mathbf{f}^{\text{ext}}, \\ \dot{\mathbf{H}}_s &= \sum \boldsymbol{\tau}^{\text{ext}}. \end{aligned} \tag{2}$$

Referring to Figure 4, where $\mathbf{f}_0^{(j)}$ are the forces and $\boldsymbol{\tau}_0^{(j)}$ are the torques measured by the sensors for the jth manipulator,

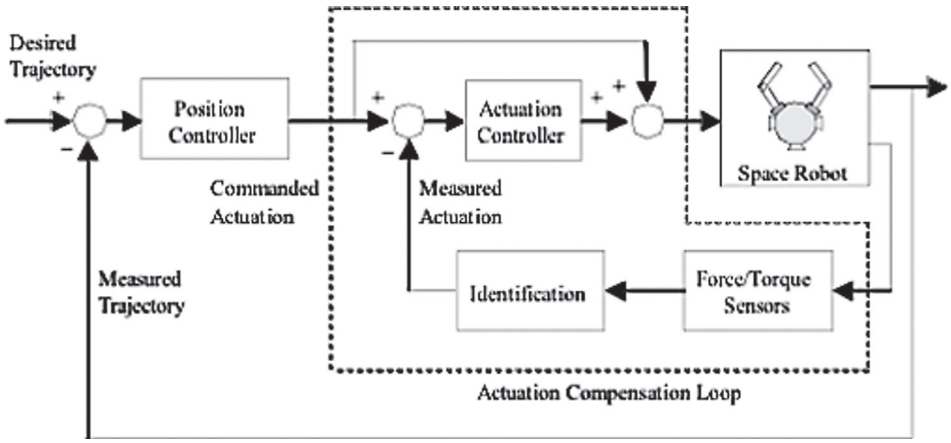

Fig. 5. The inner loop identifies and compensates for actuator efforts while the outer loop tracks the desired trajectory.

the dynamics of the spacecraft can be written as a function of the forces and torques and the measured forces and torques applied by the manipulators:

$$m_s\dot{\mathbf{v}}_s = \mathbf{f}_s - \sum_{j=1}^{p}\mathbf{f}_0^{(j)},$$

$$\mathbf{I}_s\dot{\boldsymbol{\omega}}_s + \boldsymbol{\omega}_s\times(\mathbf{I}_s\boldsymbol{\omega}_s) = \boldsymbol{\tau}_s - \sum_{j=1}^{p}(\boldsymbol{\tau}_0^{(j)} + \mathbf{r}_{s,0}^{(j)}\times\mathbf{f}_0^{(j)}), \quad (3)$$

where $\mathbf{r}_{s,0}^{(j)}$ is a vector from the center of mass of the spacecraft to the jth sensor. To find the forces and torques applied to the spacecraft, the terms are rearranged to yield:

$$\mathbf{f}_s = \sum_{j=1}^{p}(\mathbf{f}_0^{(j)} + m_s\dot{\mathbf{v}}_s,$$

$$\boldsymbol{\tau}_s = \sum_{j=1}^{p}(\boldsymbol{\tau}_0^{(j)} + \mathbf{r}_{s,0}^{(j)}\times\mathbf{f}_0^{(j)}) + \mathbf{I}_s\dot{\boldsymbol{\omega}}_s, + \boldsymbol{\omega}_s + (\mathbf{I}_s\boldsymbol{\omega}_s). \quad (4)$$

This can be rewritten to yield vectors of spacecraft forces and torques:

$$\mathbf{f}_s = \sum_{j=1}^{p}\mathbf{A}_{fs}^{(j)}(\boldsymbol{\theta})\begin{bmatrix}\mathbf{f}_0^{(j)}\\ \boldsymbol{\tau}_0^{(j)}\end{bmatrix} - f(\boldsymbol{\theta},\boldsymbol{\omega}_s,\dot{\boldsymbol{\omega}}_s,\dot{\mathbf{v}}_s),$$

$$\boldsymbol{\tau}_s = \sum_{j=1}^{p}\mathbf{A}_{\tau s}^{(j)}(\boldsymbol{\theta})\begin{bmatrix}\mathbf{f}_0^{(j)}\\ \boldsymbol{\tau}_0^{(j)}\end{bmatrix} - f(\boldsymbol{\theta},\boldsymbol{\omega}_s,\dot{\boldsymbol{\omega}}_s,\dot{\mathbf{v}}_s), \quad (5)$$

with the $\mathbf{A}$ matrices given by

$$\mathbf{A}_{fs}^{(j)}(\boldsymbol{\theta}) = [\mathbf{1} \quad \mathbf{0}],$$

$$\mathbf{A}_{\tau s}^{(j)}(\boldsymbol{\theta}) = [\mathbf{S}_{s,0}^{(j)} \quad \mathbf{1}], \quad (6)$$

where $\mathbf{1}$ is the identity matrix and $\mathbf{0}$ is the zero matrix. The skew-symmetric matrix $\mathbf{S}_{a,b}$ denotes the cross-product, $\mathbf{S}_{a,b}\,\mathbf{f} \equiv \mathbf{r}_{a,b}\times\mathbf{f}$, where $\mathbf{r}_{a,b}$ is a vector from point a to point b, and $\mathbf{S}_{s,0}^{(j)}$ is therefore the cross-product matrix from the origin of the spacecraft to the origin of the force/torque sensor for the jth manipulator.

In addition to the estimating the forces and torques applied to the spacecraft, the joint torques can be estimated. To calculate the applied joint torques, the dynamics of the links in the manipulator are included in the formulation. Since the links all belong to the same manipulator, the superscript j has been dropped to simplify the notation. Writing the relationship to find the forces $\mathbf{f}_{ci}$ and torques $\boldsymbol{\tau}_{ci}$ at the center of mass of ith link in the system yields:

$$\mathbf{f}_{c\,i} = m_i\dot{\mathbf{v}}_{c\,i} = \sum\mathbf{f}_{c\,i}^{\text{ext}},$$

$$\boldsymbol{\tau}_{c\,i} = \mathbf{I}_i\dot{\boldsymbol{\omega}}_i + \boldsymbol{\omega}_i\times(\mathbf{I}_i\boldsymbol{\omega}_i) = \sum\tau_{ci}^{\text{ext}}. \quad (7)$$

The forces at the ith joint $\mathbf{f}_i$ can be calculated (with $\mathbf{f}_0$ measured by the manipulator force/torque sensor):

$$\mathbf{f}_i = \mathbf{f}_0 - \sum_{k=0}^{i-1}\mathbf{f}_{ck}. \quad (8)$$

Similarly, the torques at the ith joint $\boldsymbol{\tau}_i$ can be calculated:

$$\boldsymbol{\tau}_i = \boldsymbol{\tau}_0 - \mathbf{r}_{0,i}\times\mathbf{f}_0 - \sum_{k=0}^{i-1}(\boldsymbol{\tau}_{ck} + \mathbf{r}_{ck,i}\times\mathbf{f}_{ck}), \quad (9)$$

where $\mathbf{r}_{0,i}$ is a vector from the origin of the force/torque sensor (the zeroth joint) to the origin of the ith joint, and $\mathbf{r}_{c\,k,i}$ is a vector from the center of mass of the kth link to the origin of the ith joint. This torque is projected onto the axis of the joint to calculate the applied joint torque:

$$\tau_{\text{a}i} = \mathbf{z}_{i-1}^{\text{T}}\tau_i, \quad (10)$$

where $\mathbf{z}_{i-1}$ is a unit vector aligned with the axis of the joint's rotation. Equations (7)–(10) are combined and the superscript notation indicating the manipulator number is again shown to yield a vector of joint torques of the form:

$$\boldsymbol{\tau}_a^{(j)} = \mathbf{A}_{\tau a}^{(j)}(\mathbf{q}^{(j)},\boldsymbol{\theta})\begin{bmatrix}\mathbf{f}_0^{(j)}\\ \boldsymbol{\tau}_0^{(j)}\end{bmatrix} - f(\boldsymbol{\theta},\mathbf{q}^{(j)},\dot{\mathbf{q}}^{(j)},\ddot{\mathbf{q}}^{(j)},\boldsymbol{\omega}_s,\dot{\boldsymbol{\omega}}_s,\dot{\mathbf{v}}_s), \quad (11)$$

where each row i of $\mathbf{A}_{\tau a}^{(j)}$ is given by

$$\mathbf{A}_{\tau ai}^{(j)} = (\mathbf{z}_{i-1}^{(j)})^{\text{T}}\,\mathbf{S}_{i-1,0}^{(j)} + (\mathbf{z}_{i-1}^{(j)})^{\text{T}} \quad (12)$$

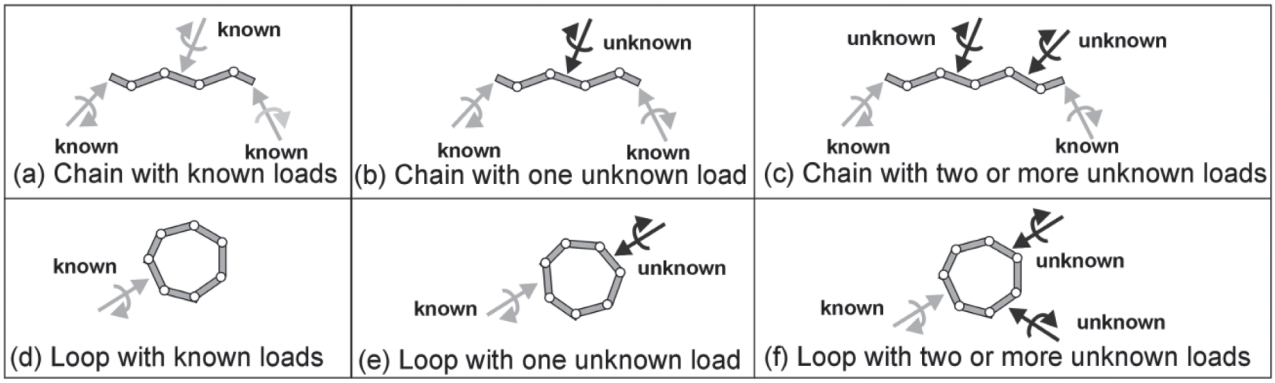

Fig. 6. Canonical system elements.

and $\mathbf{S}_{i-1,0}^{(j)}$ is the cross-product matrix from the origin of the $(i–1)$th joint to the origin of the force/torque sensor for the jth manipulator. The **A** matrices are relatively simple to derive and require minimal computation for generating the actuator estimates. When large external forces are absent and joint accelerations and velocities are relatively low, such as for a free-flying robot performing precision motions, the forces and torques can be estimated by neglecting the higher-order terms. Calculations have shown that these terms are small compared with the magnitude of the applied actuation effort, in which case Equation (11) reduces to

$$\hat{\boldsymbol{\tau}}_a^{(j)} = \mathbf{A}_{\tau a}^{(j)}(\mathbf{q}^{(j)}, \boldsymbol{\theta}) \begin{bmatrix} \mathbf{f}_0^{(j)} \\ \boldsymbol{\tau}_0^{(j)} \end{bmatrix}. \tag{13}$$

Similarly the estimates for the net thruster forces and torques become

$$\begin{aligned} \hat{\mathbf{f}}_s &= \sum_{j=1}^{p} \mathbf{A}_{fs}^{j}(\boldsymbol{\theta}), \begin{bmatrix} \mathbf{f}_0^{(j)} \\ \boldsymbol{\tau}_0^{(j)} \end{bmatrix}, \\ \hat{\boldsymbol{\tau}}_s &= \sum_{j=1}^{p} \mathbf{A}_{\tau s}^{j}(\boldsymbol{\theta}), \begin{bmatrix} \mathbf{f}_0^{(j)} \\ \boldsymbol{\tau}_0^{(j)} \end{bmatrix}. \end{aligned} \tag{14}$$

Thus, under the above assumptions the estimates of the applied joint torques and the net thruster forces and moments can be calculated from the force torque signals and the kinematic configuration of the system. Using these calculated values in closed-loop controllers actuation errors (such as joint friction and thruster imprecision) can be mitigated (Dubowsky and Papadopoulos 1993).

2.3. Minimal Sensor Architectures

Here we study the best placement and the minimum number of SBSC force/torque sensors for a given space robot to simultaneously measure joint and spacecraft actuation. The problem could also be solved by exhaustive analysis. However, given the number of manipulators, the number of links, reaction thrusters, payloads, and possible locations for the force/torque sensors, the number of cases that need to be considered could be very large. In this work it was recognized that most cases are topologically similar and the space of possible solutions can be reduced to a small number of similar cases called canonical elements. The dynamic analysis is needed only for these elements and the results can be applied to more general systems.

This observation is used here by first dividing the system at each six-axis force/torque sensor into subsystems (Boning and Dubowsky 2006b). The subsystems can be categorized by a small set of canonical elements (or canonical kinematic chains). Then, the structure of the canonical element's dynamic equations is analyzed to determine whether the boundary forces and torques acting in the elements can be determined. Finally, the results are applied to the original system to find the minimum number of sensors required to calculate the manipulator joint efforts and resultant forces moments from the spacecraft thrusters and reaction wheels.

2.3.1. Canonical Element Categorization All of the subsystems created by isolating sections for the space robots at the force/torque sensors can be reduced to the canonical elements in Figure 6. Clearly, the force/torque sensors can measure the forces and moments at the boundaries between canonical elements. Hence, the canonical elements for a system are found:

- The system is divided at the force/torque sensors.
- The sensors are replaced with equal and opposite known force/torques.
- Zero end loads at the end-effectors are replaced with known force/torques (clearly a zero load is a known load). Adding these zero loads allows more cases to be considered as one type.
- Reaction thrusters are replaced with unknown force/torques.

Finally

- Branches are replaced with chains.

Note that a known load (force and/or torques) applied at the end of a chain is equivalent to a known load applied at the branching point. The same is true for an unknown load. This procedure is summarized in Figure 7.

An example of the application of these rules is given in Figure 8, showing how the unknown reaction thrusters

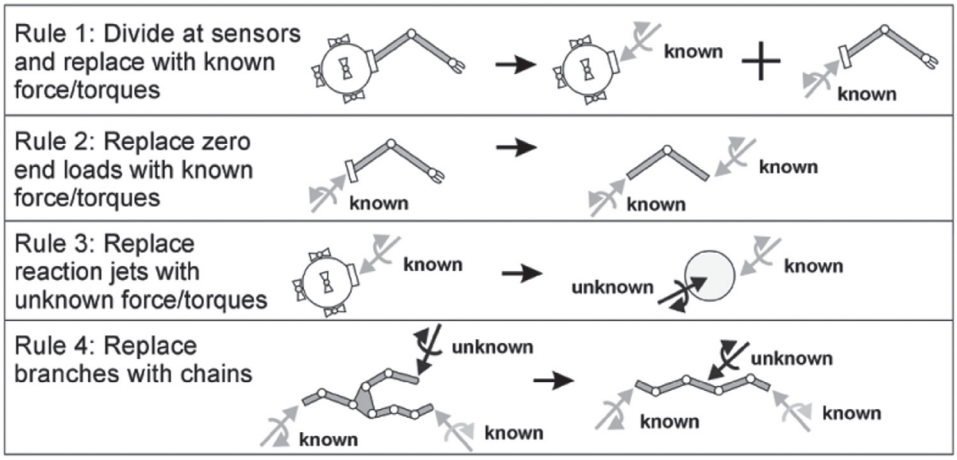

Fig. 7. System reduction to canonical elements.

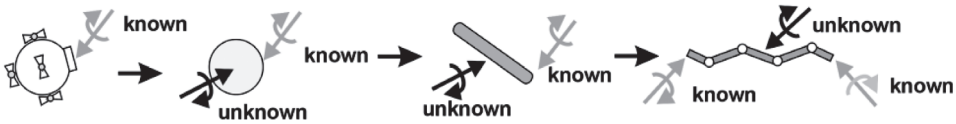

Fig. 8. Reduction of unknown reaction thrusters to chain with one unknown.

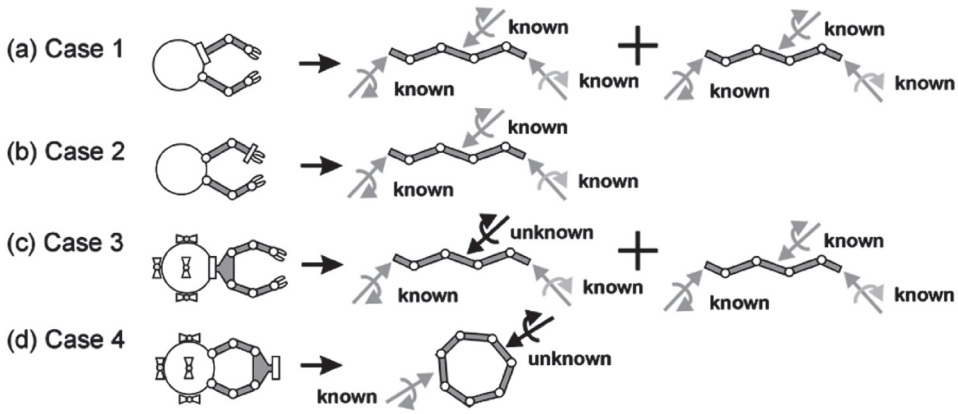

Fig. 9. More reduction examples.

on a spacecraft become the canonical element chain with one unknown. Figure 9 shows more examples. Figure 9(a) (Case 1) is a free-floating (no thrusters) space robot with two manipulators and a single force/torque sensor. The sensor separates the system into two canonical elements, both chains with known loads. Figure 9(b) (Case 2) shows a free-floating robot with a single sensor at the wrist, equivalent to a chain with known loads. The sensor measures very little, because there is no payload in this case. Figure 9(c) (Case 3) shows a free-flying space robot with a single sensor between the spacecraft and both manipulators. Figure 9(d) (Case 4) shows a free-flying space robot that contains a closed kinematic chain or loop.

2.3.2. Structure of System Dynamic Equations The objective of this section is to determine whether enough sensory information exists for a given space robot's topology to find the net actuator forces and moments on all joints and links in the system, including those produced by the robot's manipulator actuators, attitude control thrusters and reactions wheels. This also includes friction at unactuated joints.

The analysis is developed here for a full three-dimensional system such as that shown in Figure 4. Figure 10 shows a typical link, and Figure 11 shows a link at a branch point, classically called a ternary link.

When there are two unknown forces (such as in Figure 10), the forces and torques cannot be calculated directly. Starting calculations at several points in the chain and propagating the known forces and moments to a common point often permits the problem to be solved. In other cases, additional information, such as that provided by an additional force/torque sensor, is needed to permit a solution. When all of the links in the system have been visited, it is possible to determine whether the

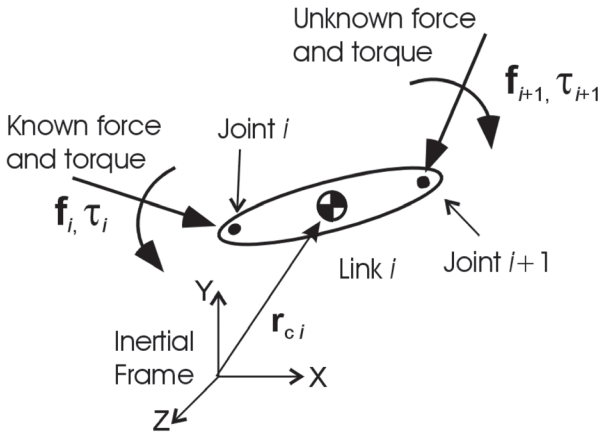

Fig. 10. Link with one unknown load.

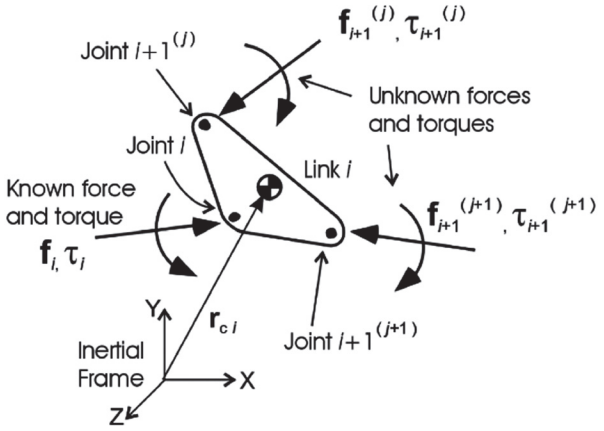

Fig. 11. Link with two unknown loads.

given set of sensors is sufficient or additional sensors are required.

2.3.3. Analysis of Canonical Elements The above analysis can be applied case by case to the canonical elements in Figure 6. First, consider the chain with known loads, as in Figure 6(a). By starting with the link on the far left, finding the actuator torques on the first joint is possible. Continuing with the links from left to right, calculation can yield the forces and torques on all joints in this system. Hence, enough sensors exist to completely identify all actuation efforts for this case.

The canonical element chain with one unknown load also has enough sensors, but working inward from both ends of the chain simultaneously is necessary so that the single unknown load at the middle link can be determined. However, for any chain that has more than one unknown load, as in Figure 6(c), all actuator efforts cannot be determined without adding more sensors.

Loops can be resolved into two chains joined by two branching links. Loops are analyzed by starting with a link that has only known applied loads and propagating the loads in both directions around the loop until the chain rejoins. Enough sensors do not exist to determine all actuation efforts for any of the three canonical elements with loops. However, inserting a sensor in a loop converts this problem into the case of the chain with known loads (see Figure 6(a)). To summarize, for all of the canonical elements, only a chain with known loads, as in Figure 6(a), and a chain with one unknown load, as in Figure 6(b), have enough sensory information to determine all actuation efforts.

By using the analysis of the canonical elements, applying the results to the original system to determine sensor placement is straightforward. For any given robot configuration with multiple manipulators, links, branches, etc., it is possible to enumerate potential sensor placements, divide the system into subsystems at the sensors, classify each subsystem by its canonical element, eliminate the layouts where not enough sensory information exists, and find the minimal number and placement of sensors for the system.

2.3.4. Minimum Sensor Configurations The above sensor placement method is applied to space robots with one and two manipulators. Figure 2 shows systems such as that depicted in Figure 4 studied to determine the torques at each joint and the reaction thruster forces. (The parameters varied are number of manipulators ($p = 1, 2$), number of links per manipulator ($n = 1, 2, \ldots$), whether they have reaction thrusters (free-flying or free-floating), and whether a manipulator has payload or not.) The force/torque sensors maybe located at the manipulator wrist and or the manipulator's base (where it is mounted to the spacecraft). For most cases, enumerating the cases where the sensor is placed at any joint of a manipulator between its two ends is unnecessary, because the cases can be shown to be equivalent to the cases with sensors placed at the ends of a manipulator.

A collection of single manipulator cases, with and without thrusters, is summarized in Figure 12. For all cases with a single manipulator, adequate sensing exists with one sensor placed at either end of the manipulator. Figures 12–16 summarize the results for space robots with two manipulators. The cases in Figure 13 are free-floating (cases with no active thrusters). The first row in these figures shows the possible sensor placements when only one sensor is available. The sensor can be placed between the manipulator and the spacecraft, at the end-effector, between both manipulators and the spacecraft, or at both end-effectors. The second row shows placement of two sensors, the third row shows placement of three sensors, and the last row shows the only possible configuration with four sensors.

All of these cases reduce to the canonical chain elements with at most one unknown load, except for the two loop cases that are crossed out. These cases do not have enough sensing to determine all actuation efforts. For the remaining cases that have enough information, determining the minimal number of sensors (one) and its potential locations is straightforward. These cases are outlined in bold. Figure 14 shows the same cases as Figure 13, except that the space robots now have thrusters. The addition of the unknown thruster loads does not change the results; there are still only two cases that do not have enough sensing, and a single force torque sensor is enough to measure all of the actuator outputs.

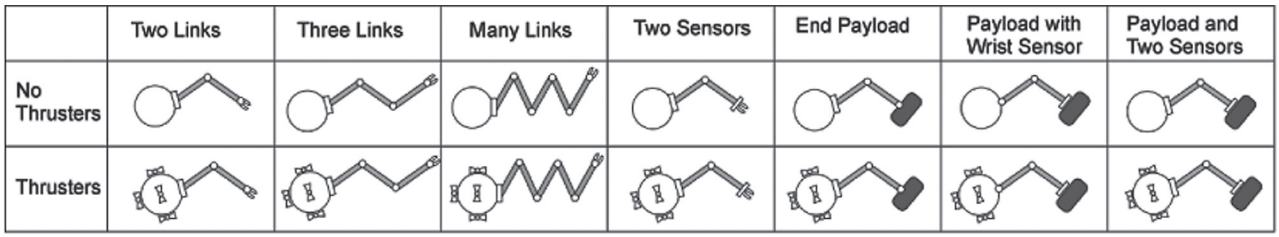

Fig. 12. Space robot configurations for a single manipulator.

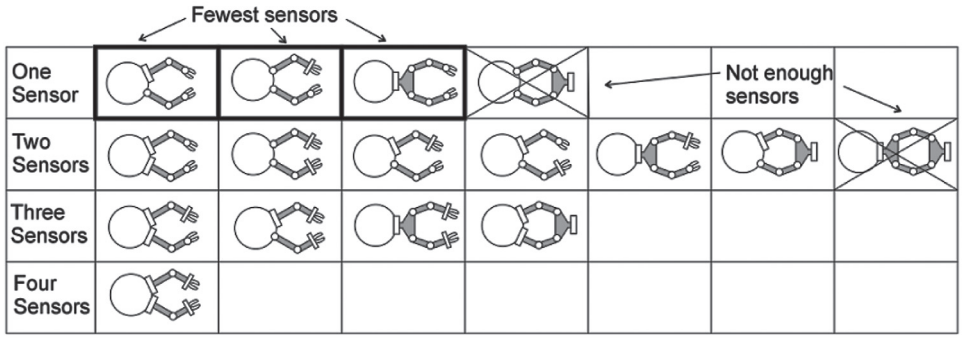

Fig. 13. Space robot configurations for two manipulators and no thrusters.

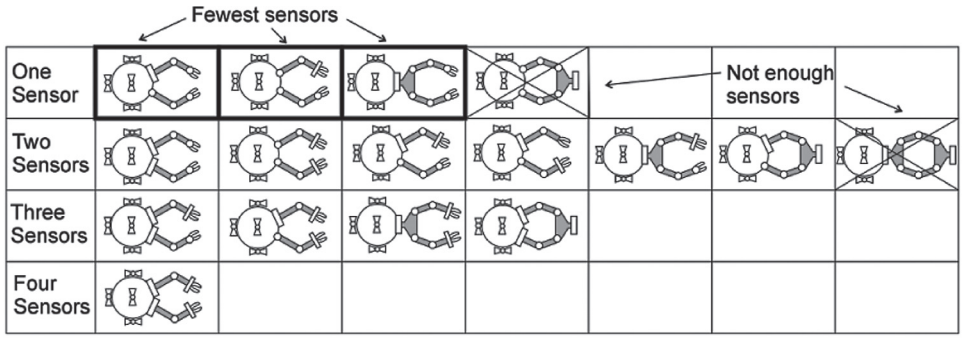

Fig. 14. Space robot configurations for two manipulators and thrusters.

Figure 15 shows robots without thrusters but carrying a payload grasped by both manipulators, creating a closed loop. Most of the loops are broken by a sensor, so that the actuator efforts can be measured, but there are two places for a single sensor to determine actuation. Figure 16 shows the robots from Figure 15 with thrusters. Once again, the addition of unknown thruster forces does not change the results.

These results provide a guide for selecting system kinematic configurations that require the minimum number of sensors to measure the systems actuator efforts and hence will be capable of more precise control performance. Of course, other important issues need to be considered in designing a system's kinematic structure, including the workspace, dexterity, and so on. In addition, in some cases additional sensors beyond the minimum number might be desirable to provide redundancy. Knowing the sensor minimum set provides guidance to these design choices.

3. Simulation Studies

3.1. System Description

Simulation studies were performed to demonstrate the effectiveness and validity of the control model using a small number of SBSC sensors. In the results presented here, SBSC is applied to the two-manipulator robot performing a satellite capture mission (Boning 2009). It is assumed that the satellite has lost its attitude control due to a component failure, or it has run out of attitude control fuel and is spinning out of control. It needs to be captured, repaired or de-orbited. The robot has two manipulators performing the pre-grasp portion of the satellite capture task. When the robot gets close enough to the satellite, the robot's manipulator tracks and reaches for a hardened grasping point on the satellite, such as the payload attachment ring. The objective of the task is for the robot to track the spinning grasp point (within a specified position and orientation error) long

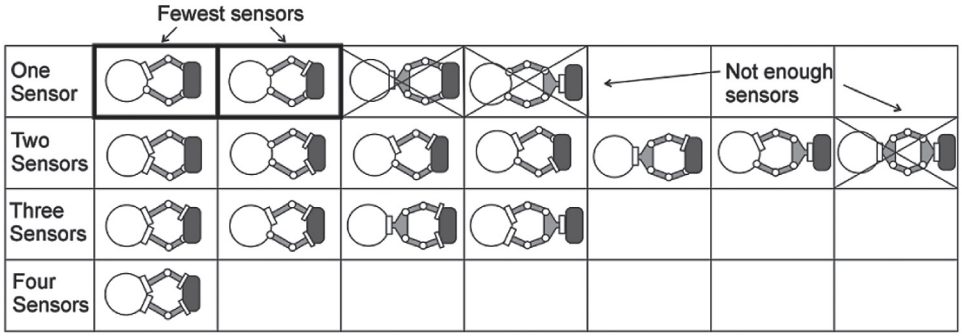

Fig. 15. Space robot configurations for two manipulators and a payload.

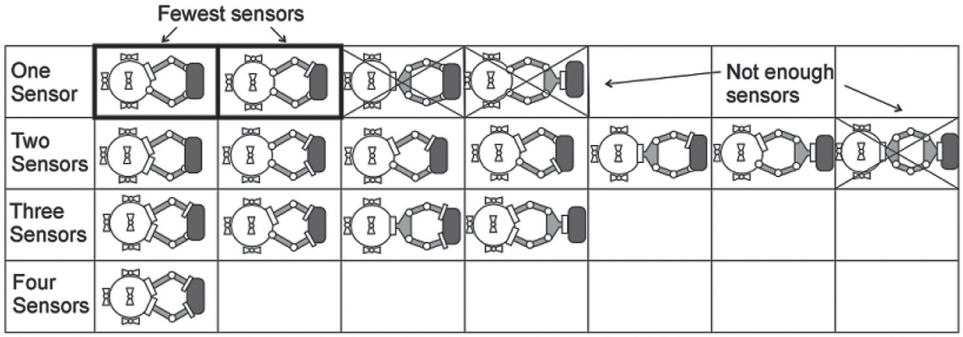

Fig. 16. Space robot configurations for two manipulators, a payload, and thrusters.

Table 1. Space Robot Parameters

	Length (m)	Mass (kg)	Inertia (kg m^2)
Spacecraft	4.2 (diameter)	2,400	5,808
Link 1	4	200	345
Link 2	3	100	106

enough to allow the robot's end-effector to make a firm grasp. It is assumed that the relative position and orientation between the robot's end-effector and the grasp point can be measured. The robot's inertial parameters are assumed to be well known, but the joint friction and the thruster gains are not well known.

Table 1 shows the system parameters used in the simulations discussed in the following. These values are based on projected space robotic system designs (Newman et al. 1992; Oda et al. 2003). Each manipulator has two links and the manipulator mounting points are separated by 90°. The joint friction is assumed to be a Coulomb friction with magnitudes approaching 20–50% of the combined joint–actuator's maximum torque. The characteristics of the thruster errors are assumed to be unknown. The target satellite has a radius of 3 m, and it is assumed to be spinning with an angular velocity $\boldsymbol{\omega}_t$ of three revolutions per minute. The positions of the end-effectors are controlled by a Jacobian transpose controller during this task. The robot needs to avoid firing its thrusters in the direction of the satellite (Matsumoto et al. 2003).

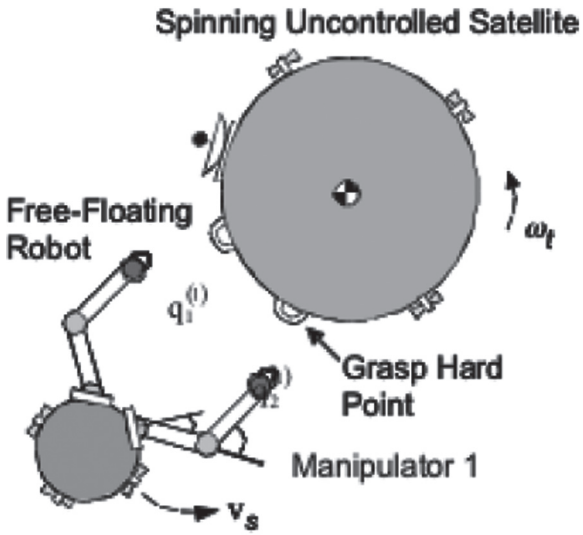

Fig. 17. Flat spin satellite capture example.

Figure 17 shows one force/torque sensor at the base of each arm manipulator. One force/torque sensor would provide the required information to estimate the joint torques of both manipulators and the forces of the attitude control thruster. Such a redundant two-sensor configuration would make the systems robust to a single sensor failure. In the simulation results presented here, sensor failures are not included and hence the redundant sensor is not required. During the capture task, the robot fires its thrusters at the

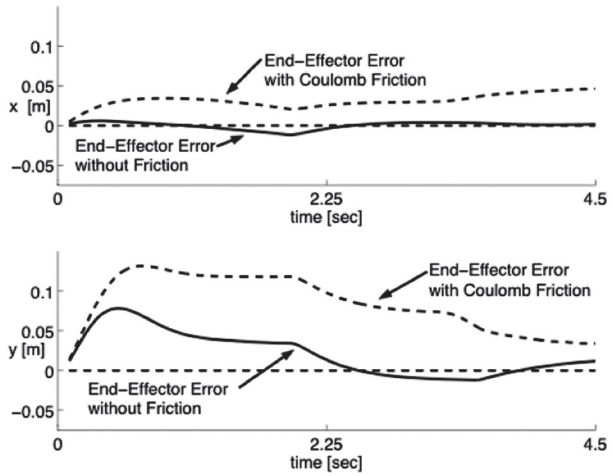

Fig. 18. Manipulator 1 end-effector position errors.

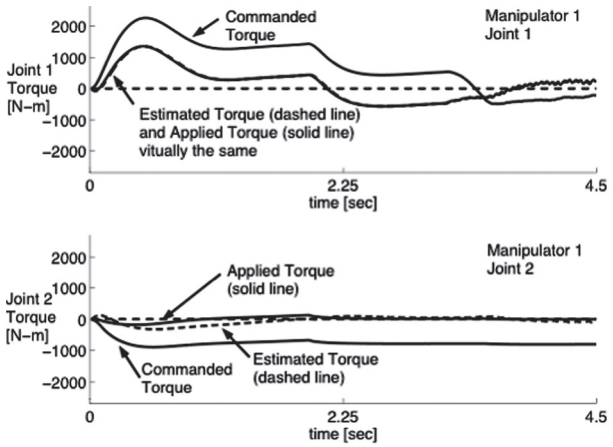

Fig. 19. Manipulator 1 torques for the large satellite capture task.

same time as the manipulator end-effectors are tracking the grasp points.

3.2. Tracking Performance

Figure 18 shows the manipulator end-effector position errors in the x and y directions for one of the manipulators. The solid curves shows the position errors when there is no joint friction, and the dashed curves show the position errors when there is Coulomb friction in all of the manipulator joints. Clearly, the errors are larger when the joint torques are corrupted by friction. There is no torque control loop active for this case. Hence, there is no compensation for the joint friction.

Figure 19 shows the torques in the joints of manipulator as commanded by the position controller and the actual joint torques that are a combination of the commanded torques and the joint friction. The dashed line shows the torque estimated using base force/torque sensor signals and the SBSC algorithm. It can be seen that for joint 1 SBSC give a very good estimate of the actual applied torque. Figure 19 also shows the estimates for the second joint, but they are not as good as for the first joint. This is because the results presented here are for a simple form SBSC that neglects the acceleration in the dynamic model and therefore gives the best estimates for actuations closest to the base sensor. These estimates can easily be used as feedback signals in a closed torque controller to mitigate the degrading effects of the joint friction (Boning 2009).

The spacecraft forces and moments can be estimated simultaneously as the joint torques using the same sensor and the SBSC algorithm. Figure 20 shows the spacecraft forces in the x and y directions. The figure also shows the commanded forces, the actual applied forces, and the SBSC estimate values. The actual force values experienced by the spacecraft are substantially different to the commanded values. However, the method provides good agreement between the estimated actuation value and the actual

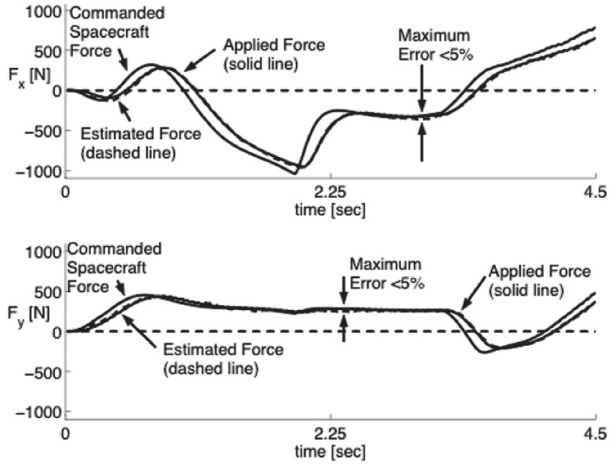

Fig. 20. The x and y thruster forces for the large satellite capture task.

value. The error between the estimate and the actual values is less than 5%.

The above simulation results show that the SBSC algorithm using the minimum one force/torque sensor is able to estimate both the joint torques, including important frictions, and the thruster forces with good accuracies. With these sensor-based estimates it is straightforward to close torque and force loops on the manipulator and spacecraft actuator efforts and thereby mitigate the effects of both joint friction and thruster imprecision.

4. Conclusions

The control performance of robots in orbit can be significantly degraded by the imprecision of their actuators, particularly joint friction in their manipulators and errors in their spacecraft's attitude control thrusters. Sensing is key to reducing the degrading effect of these factors. A method called space base sensor control (SBSC) has been presented that permits a space robot's manipulator and spacecraft

actuator efforts to be estimated from the use of force/torque sensors mounted in the kinematic structure of the system. These sensors can be used to estimate friction in the space robots manipulator joints and the errors in its spacecraft attitude control thrusters. Using these estimates in inner actuator control feedback loops the effects of joint friction and spacecraft thruster inaccuracies can be mitigated.

However, sensing adds system complexity, weight, and cost, so minimizing the number of sensors is important. This paper has shown that minimum sensor configurations exist that will provide the information required for identifying a system actuation and provided guides to finding these configurations.

Acknowledgments

This work was sponsored by the Japan Aerospace Exploration Agency (JAXA) and the Department of Mechanical Engineering at MIT.

References

Boning, P. (2009). *The Coordinated Control of Space Robot Teams for the On-Orbit Construction of Large Flexible Space Structures*, PhD Thesis, Department of Mechanical Engineering, MIT.

Boning, P., Ono, M., Nohara, T. and Dubowsky, S. (2008). An experimental study of the control of space robot teams assembling large flexible space structures. *Proceedings of the 9th International Symposium on Artificial Intelligence, Robotics and Automation in Space (i-SAIRAS 2008)*, Pasadena, CA, 26–29 February 2008.

Boning, P. and Dubowsky, S. (2006a). Identification of actuation efforts using limited sensory information for space robots. *Proceedings of the 2006 IEEE International Conference on Robotics and Automation*, May 2006.

Boning, P. and Dubowsky, S. (2006b). A study of minimal sensor topologies for space robots. *10th International Symposium on Advances in Robot Kinematics*, Ljubljana, Slovenia, June 2006.

de Wit, C. (1988). *Adaptive Control of Partially Known Systems: Theory and Applications*. Boston, MA, Elsevier.

de Wit, C., Olsson, H., Astrom, K. J. and Lischinsky, P. (1995). A new model for control of systems with friction. *IEEE Transactions on Automatic Control*, 40(3): 419–425.

Dubowsky, S. and Boning, P. (2007). The coordinated control of space robot teams for the on-orbit construction of large flexible space structures. *Proceedings of the 2007 IEEE International Conference Robotics and Automation, Special Workshop on Space Robotics*, Rome, Italy, April 2007.

Dubowsky, S. and Papadopoulos, E. (1993). The kinematics, dynamics, and control of free-flying and free-floating space robotic systems. *IEEE Transactions on Robotics and Automation, Special Issue on Space Robotics*, 9(5): 531–543.

Huntsberger, T., Stroupe, A. and Kennedy, B. (2005). System of systems for space construction. *IEEE International Conference on Systems, Man, and Cybernetics*, Waikoloa, HI, October 2005.

Ipri, S. and Asada, H. (1995). Tuned dither for friction suppression during force guided robotic assembly. *IEEE International Conference on Intelligent Robots and Systems*, Vol. 1, pp. 310–315.

Kawano, I., Mokuno, M., Kasai, T. and Suzuki, T. (2001). Result of autonomous docking rendezvous experiment of engineering test satellite ETS-VII. *Journal of Spacecraft and Rockets*, 38(1).

Lillie, C. (2006). On-orbit assembly and servicing for future space observatories. *Space 2006*, San Jose, CA, 19–21 September 2006.

Matsumoto, S., Jacobsen, S., Dubowsky, S. and Ohkami, Y. (2003). Approach planning and guidance for uncontrolled rotating satellite capture considering collision avoidance. *Proceedings of the 7th International Symposium on Artificial Intelligence and Robotics & Automation in Space: i-SAIRAS*, Nara, Japan, 2003.

Morel, G. and Dubowsky, S. (1996). The precise control of manipulators with joint friction: a base force/torque sensor model. *Proceedings of the 1996 IEEE International Conference on Robotics and Automation*, Minneapolis, MN, April 1996, Vol. 1, pp. 360–365.

Morel, G., and Dubowsky S. (1998). *High Performance Control of Manipulators Using A Base Force/Torque Sensor*. Patent Number 5,767,648, May 1998.

Morel, G., Iagnemma, K. and Dubowsky, S. (2000) The precise control of manipulators with high joint-friction using base force/torque sensing. *Automatica: The Journal of the International Federation of Automatic Control*, 36(7): 931–941.

Newman, W. S., Glosser, G. D., Miller, J. H. and Rohn, D. (1992). The detrimental effect of friction on space microgravity robotics. *Proceedings of the 1992 IEEE International Conference on Robotics and Automation*, Nice, France, May 1992, Vol. 2, pp. 1436–1441.

Oda, M. (2001). ETS-VII: achievements, troubles, and future. *Proceedings of the 6th International Symposium on Artificial Intelligence and Robotics and Automation in Space: i-SAIRAS*, Quebec, Canada, 2001.

Oda, M., Ueno, H. and Mori, M. (2003). Study of the solar power satellite in NASDA. *Proceedings of the 7th International Symposium on Artificial Intelligence, Robotics and Automation in Space, i-SAIRAS*, Nara, Japan, 2003.

Ono, M., Boning, P., Nohara, T. and Dubowsky, S. (2008). Experimental validation of a fuel-efficient robotic maneuver control algorithm for very large flexible space structures. *Proceedings of the 2008 IEEE International Conference on Robotics and Automation*, Pasadena, CA, May 2008.

Pfeffer, L. E., Khatib, O. and Hake, J. (1989). Joint torque sensory feedback of a PUMA manipulator. *IEEE Transactions on Robotics and Automation*, 5(4): 418–425.

Shoemaker, J. and Wright, M. (2004) Orbital express on-orbit satellite servicing demonstration. *Conference on Spacecraft Platforms and Infrastructure (Proceedings of SPIE*, Vol. 5419). Bellingham, WA, SPIE—International Society for Optical Engineering, pp. 57–65.

Sidi, M. (1997). *Spacecraft Dynamics and Control*. Cambridge, Cambridge University Press.

Slotine, J.-J. and Li, W. (1987). On the adaptive control of robot manipulators. *The International Journal of Robotics Research*, 6(3): 49–59.

Staritz, P. J., Skaff, S., Urmson, C. and Whittaker, W. (2001). Skyworker: a robot for assembly, inspection and maintenance of large scale orbital facilities. *Proceedings of the 2001 IEEE*

International Conference on Robotics and Automation (ICRA 2001), Seoul, Korea, May 2001, pp. 4180–4185.

Ueno, H., Nishimaki, T., Oda, M. and Inaba, N. (2003). Autonomous cooperative robots for space structure assembly and maintenance. *Proceedings of the 7th International Symposium on Artificial Intelligence, Robotics, and Automation in Space: i-SAIRAS 2003*, NARA, Japan, May 2003.

Vischer, D. and Khatib, O. (1995). Design and development of high-performance torque-controlled joints. *IEEE Transactions on Robotics and Automation*, 11(4): 537–544.

Visentin, G. and Venturini, M. (1997). Novel lightweight space robot joint actuator. *Preparing for the Future*, 7(2).

Whittaker, W., Staritz, P., Ambrose, R., Kennedy, B., Fredrickson, S., Parrish, J. and Urmson, C. (2001). Robotic assembly of space solar-power facilities. *Journal of Aerospace Engineering*, 14(2).